*Polish J. Chem.*, **76**, 1009–1018 (2002)

# Nitrogen-15 Kinetic Isotope Effects in the Decomposition of Nitric Oxide on Copper

**by S. Polič[1], M. Senegačnik[1], I. Kobal[1*] and M. Zieliński[2]**

[1]*J. Stefan Institute, 1001 Ljubljana, POB 3000, Jamova 39, Slovenia*
[2]*Jagiellonian University, 30-060 Kraków, Poland*

*(Received February 4th, 2002; revised manuscript April 15th, 2002)*

Isotopic rate constant ratios, $k_{14}/k_{15}$, have been determined for the decomposition of nitric oxide over copper wire at initial NO pressures 40–60 kPa over temperature range 725–825 K. They were interpreted using the Bigeleisen formalism. Under these experimental conditions the reaction was found to be second order in NO. On the basis of the temperature independence, $k_{14}/k_{15} = 1.010 \pm 0.001$ at all temperatures studied, a *cis* ONNO transition state was shown to account satisfactorily for the experimental $k_{14}/k_{15}$ values.

**Key words**: nitric oxide decomposition, polycrystalline copper, kinetic isotope effects, transition state

Because of increasingly stringent legislation for car emissions world wide [1], the reactivity, selectivity and operational stability of the three-way catalyst (TWC), which is designed to simultaneously convert $NO_x$, CO and unburned hydrocarbons into harmless compounds, have been studied extensively and steadily improved [2–4]. Although catalytic converters based on precious metals, such as Rh, Pt and Pd are in widespread use, more readily available and less expensive metals are sought. Recently, interest in Cu has increased, both in the form of $Al_2O_3$ supported catalysts [5] and Cu-exchanged zeolites [6,7], with Cu-ZSM-5 being the most active [8,9]. It was also shown that the addition of Cu to Pd increases the catalytic activity of the latter [10,11]. Therefore, interaction and reaction of NO with Cu are crucial processes, whose characteristics should be known in order to better understand and hence improve catalytic features.

Adsorption of NO to polycrystalline as well as to (111), (110) and (100) copper surfaces is accompanied by a charge transfer [12–15]. Both upright and bent geometries have been confirmed [14,16–20], with the N atom attached to the surface [12,18,19], although linkage *via* O cannot be excluded [12,18]. NO adspecies are stable at 85 K and dissociate above 290 K into adsorbed N and O atoms [12–15,21–26]. N adspecies recombine and desorb as $N_2$ above 395 K [26], while O adspecies are firmly bound and form $Cu_2O$ [26–28]. The mechanism of the overall reaction has not

*The author to whom correspondence should be sent: tel: 00386 1 477 35 80; fax: 00386 1 477 38 11; e-mail: ivan.kobal@ijs.si

been entirely explained. Most probably it proceeds *via* formation of an adsorbed $N_2O$ intermediate [13,14,22,24,25,29], which then dissociates, as also found in NO decomposition on Pd [30]. For the formation of a linear $N_2O(a)$, weakly linked to the surface *via* O atom, two possibilities have been proposed [25]: (i) dissociation of a weakly bound surface dimer, $(NO)_2(a) \rightarrow N_2O(a) + O(a)$, or (ii) recombination, $NO(a) + N(a) \rightarrow N_2O(a)$. $(NO)_2$ dimers have been found experimentally in gaseous [31] and condensed [32] phases, on Cu, Ag and Rh surfaces [33–35], and also predicted theoretically [33–40].

In this paper we present results on kinetic isotope effects (KIE), $k_{14}/k_{15}$ rate constant ratios, in the reaction $NO + 2Cu \rightarrow 1/2\ N_2 + Cu_2O$, measured on polycrystalline Cu at NO initial pressures 40–60 kPa between 725–825 K. This study aimed at providing geometry of the transition state of the rate-determining and isotope fractionation governing elementary step of the reaction mechanism. In the theoretical interpretation and according to proposals (i) and (ii) above, we assumed $(NO)_2$ dimer and NNO as the transition states of this elementary step.

## EXPERIMENTAL

**Apparatus**: The same Pyrex glass vacuum system was used as previously [41,42]. Its main parts are: 10 $dm^3$ vessels for storing NO and CO, traps for purifying and condensing gases, a Töpler mercury pump to measure pressures and transfer gases, and a 220–250 $cm^3$ cylindrical quartz reaction vessel ($\phi = 40$ mm) fitted with a capillary mercury manometer. The desired reaction temperature was controlled within ±1 K by an electric cylindrical kanthal furnace.

**Materials:** *Gases*. NO was obtained from the reaction of sodium nitrite with sulphuric acid in a Kipp gas evolving apparatus [43]. Uncondensed impurities were removed by repeated condensation at liquid nitrogen temperature, followed by evacuation and sublimation. $NO_2$, $N_2O_3$ and water were removed by several vacuum sublimations at 156 K (ethyl alcohol in liquid nitrogen). Mass spectrometric analysis of the purified NO showed no argon or $NO_2$. CO of 99.9 vol. % purity (L'air Liquide, France) was used without further purification.

*Copper.* Reagent grade (99.9%) electrolytic copper wire of 0.2 mm diameter (SAFI, Milano, Italy) was used. In order to facilitate handling, the wire was shaped into *ca*. 40 cm long spirals with a diameter of *ca*. 0.4 cm. About 100 g of spirals with a total surface area of about 2.5 $dm^2$ were degreased for 20 hours with benzene in a reflux apparatus and then introduced into the reaction vessel. Two kinds of Cu treatment were applied: (a) spirals were degreased as described above (Cu-a sample), and (b) spirals, degreased as above, were further subjected to NO at 725–825 K to form a 0.8–1.0 μm thick surface $Cu_2O$ layer, which was then quantitatively reduced by CO at 675 K (Cu-b sample). Thus, NO decomposition took place on a compact Cu layer on Cu-a samples, but on a porous spongy Cu layer on Cu-b samples. Prior to each kinetic or KIE experiment, the spirals were degassed for an hour at 675 K to a background pressure of about 10 mPa.

**Procedures:** *Kinetic runs***.** Because under our experimental conditions $N_2O$ was not found in the residual gas phase, the reaction $NO + 2Cu \rightarrow 1/2\ N_2 + Cu_2O$ is accompanied by a volume change. Its time course was followed by recording the total pressure in the reaction vessel, taking into account the relationship $P_{NO} = 2P - P^0_{NO}$, where $P$ is the total pressure at time t, and $P^0_{NO}$ and $P_{NO}$ are NO partial pressures at time 0 and t, respectively. NO was introduced into the reaction vessel at room temperature, the vessel was heated to and kept at the desired temperature and the pressure measured by the capillary manometer. The reaction was stopped by removing the furnace and cooling the reaction vessel to room temperature. Kinetics were studied on both Cu-a and Cu-b samples.

*KIE determinations*. Nitrogen-15 kinetic isotope effects, $k_{14}/k_{15}$, were determined on Cu-b samples at 725, 775 and 825 K. Prior to each run, the spirals were degassed. If NO decomposition became significantly slower due to formation of a $Cu_2O$ layer, the spirals were regenerated by CO. NO was introduced to an initial pressure, $P^0_{NO}$, of 40–60 kPa at room temperature, measured using the Töpler pump. The reaction vessel was heated to and kept at the desired temperature. After more than 70% NO decomposition, the reaction was stopped by removing the furnace and cooling the vessel to room temperature. By means of the Töpler mercury pump the reaction gas mixture was pumped back and forth through a trap cooled with liquid nitrogen in order to freeze out residual NO and separate it from $N_2$. The NO was purified by repeated sublimation. The final NO pressure, $P^f_{NO}$, was measured by the Töpler pump at room temperature, and the extent of reaction, $f$, obtained from the expression: $f = 1 - P^f_{NO}/P^0_{NO}$. The NO was then sealed into a glass ampoule and stored for isotopic analysis on a Nier-M$^c$Kinney type double collector mass spectrometer [41,42] to determine the isotopic mass ratios $R_0 = [^{15}N^{16}O]_0/[^{14}N^{16}O]_0$ and $R_f = [^{15}N^{16}O]_f/[^{14}N^{16}O]_f$ in the initial and residual NO, respectively. The relative standard deviation in $R$ was usually below ±0.5%.

Kinetic isotope effects were calculated by applying the formula [44–46]:

$$\frac{k_{14}}{k_{15}} = \left(1 + \frac{\log(R_f/R_0}{\log(1-f)}\right)^{-1}$$

## RESULTS AND DISCUSSION

**Kinetics**: The kinetics of formation of coherent oxide layers generally obey the parabolic rate law [47] which, in our static system, was expressed by:

$$v = \frac{-dP_{NO}}{dt} = S\frac{k_O P^n_{NO}}{n_O} \quad \text{or in the logarithmic form: } \log v = \log S + \log k_O + n\log P_{NO} - \log n_O$$

where $v$ is the rate of oxidation, $S$ is the sample surface area (2.5 dm$^2$), $n_O$ the number of moles of O atoms involved in $Cu_2O$ formation (equal to the number of moles of NO consumed) per unit area, and $k_O$ and $n$ are the parameters defining the parabolic rate constant, $k_p = k_O P^n_{NO}$. Decreases of NO partial pressure on compact Cu layers (Cu-a sample) in four consecutive reactions at 775 K are shown in Fig. 1. The rate is suppressed by increasing the thickness of the $Cu_2O$ layer. If slopes of tangents to the curves in Fig. 1 at selected NO pressures are plotted versus $n_O$, calculated from the consumption of NO, the straight lines in Fig. 2 are obtained, confirming the parabolic rate law with $n = 2.0 \pm 0.3$.

For decomposition on the porous Cu layers (Cu-b sample) at 775 K, $1/P_{NO}$ was plotted *versus* time $t$. Four consecutive runs are shown in Fig. 3. Straight lines indicate the second order kinetics in NO, expressed by:

$$\frac{1}{P_{NO}} - \frac{1}{P^0_{NO}} = k_2 t$$

where $k_2$ is the second-order rate constant. The rate was not decreased with increasing the thickness of the porous Cu layer, indicating that the rate-determining step is one of the surface reactions at the $Cu_2O$/NO interface, and not diffusion of reactants.

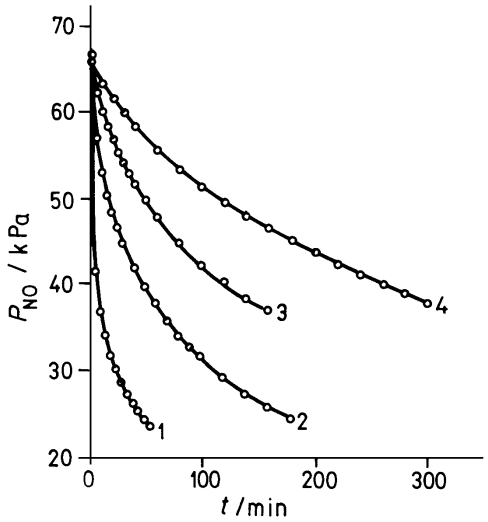


**Figure 1.** Decrease of NO partial pressure, $P_{NO}$, during consecutive decompositions of NO on Cu at 775 K. Value of $n_O$/mmol m$^{-2}$ (see text) before each run is: **1**) 1.9, **2**) 9.4, **3**) 19.2 and **4**) 40.

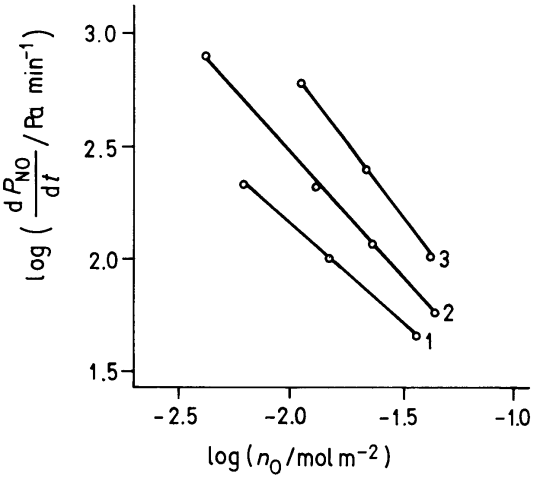


**Figure 2.** Logarithm of rate of NO decomposition on Cu at 775 K *versus* log $n_O$ at $P_{NO}$/kPa =: **1**) 25, **2**) 40 and **3**) 55.

**Kinetic isotope effects**: Values of temperature, extent of reaction, isotopic ratio and nitrogen kinetic isotope effects are listed in Table 1. The latter are temperature independent, the average being $1.011 \pm 0.001$ at all three experimental temperatures. As in our previous work, the results were interpreted using the Bigeleisen's formula to calculate the harmonic rate ratios [44,46,48]:

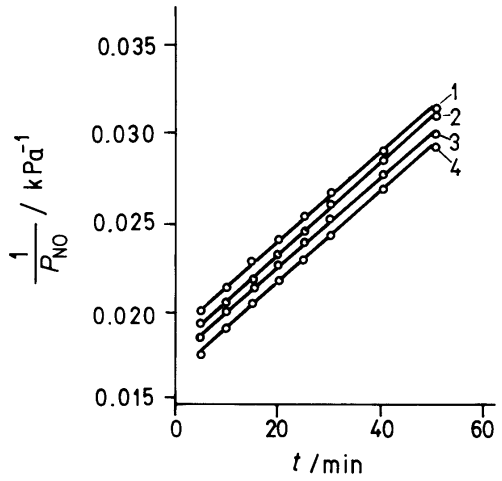


**Figure 3.** Reciprocal $P_{NO}$ *versus* time for four consecutive decompositions, 1–4, of NO on Cu at 775 K over a 0.8–1.0 μm thick $Cu_2O$ layer.

$$\frac{k_{14}}{k_{15}} = \frac{\nu_{L14}^{\neq}}{\nu_{L15}^{\neq}} \prod_{j=1}^{3n-6} \frac{u_{15j} \sinh(u_{14j}/2)}{u_{14j} \sinh(u_{15j}/2)} \prod_{j=1}^{3n^{\neq}-7} \frac{u_{14j}^{\neq} \sinh(u_{15j}^{\neq}/2)}{u_{15j}^{\neq} \sinh(u_{14j}^{\neq}/2)}$$

in which ≠ denotes the transition state. The first product includes the isotopic frequencies of the NO reactant molecule, available from the literature [32], and the second one the real frequencies of the transition state, which were obtained by applying Wilson's ***FG*** method [48,49]. $\nu_L$ is the frequency of the normal mode belonging to the reaction coordinate, and $u = hc\omega/k_BT$ ($\omega$ – wave number, h – Planck's constant, $k_B$ – Boltzmann's constant, $c$ – speed of light, $T$ – temperature). According to the above proposed alternatives (i) and (ii) for the reaction mechanism [25], we assumed ONNO and NNO structures as possible transition states. Because $(NO)_2$(a) and $N_2O$(a) were found to be only weakly bound to the surface [25], interaction of the transition state with Cu atoms has not been taken into account in our calculations [46].

*ONNO transition state.* Internal co-ordinates were defined (see inset in Fig. 4) [32,48] as changes of the N–N and N–O bond lengths ($D$ and $d$, respectively), of the interbond angle α between N–N and each of the two N–O bonds, and of the torsional angle τ, which is the twisting angle between the two N–O bonds around the N–N axis. Accordingly, force constants, elements of the ***F*** matrix, were defined [48]. In order to obtain $\nu_L = 0$ as the result of a zero determinant of ***F***, the following conditions were imposed in solving the ***FG*** matrix equation [49]: a) $F_{Dd} = (F_D F_d/2)^{1/2}$ with $F_{dd} = 0$, b) $F_{Dd} = +(F_D F_d)^{1/2}$ with $F_{dd} = 0$, c) $F_{Dd} = -(F_D F_d)^{1/2}$ with $F_{dd} = 0$, and d) $F_{dd} = -F_d$ with $F_{Dd} = 0$, thus describing the reaction co-ordinate in four different ways. In our calculations, $F_D$ and $F_d$ were varied in ranges of 100–1900 $Nm^{-1}$ and 100–1500 $Nm^{-1}$, respectively (both in steps of 100 $Nm^{-1}$), α in the range 100–160° (in steps of 5°). $F_\alpha$ was

fixed successively at 60, 80 and 100 $Nm^{-1}$, while τ and $F_\tau$ were fixed at 0° and 20 $Nm^{-1}$, respectively. For a selected value of the stretching force constant, the related bond length was calculated applying semi-empirical relationships [50–52]. Selected results for 775 K are presented in Fig. 4.

**Table 1.** Temperature, extent of reaction, isotopic ratios and experimental $k_{14}/k_{15}$ values for NO decomposi*tion on Cu.*

| *T/K* | *f* | $R_f/R_0$ | $k_{14}/k_{15}$ |
|---|---|---|---|
| 725 | 0.970 | 1.041 | 1.011 |
| 725 | 0.832 | 1.021 | 1.012 |
| 725 | 0.842 | 1.021 | 1.011 |
| 725 | 0.900 | 1.022 | 1.010 |
| 725 | 0.876 | 1.021 | 1.010 |
| 725 | 0.881 | 1.024 | 1.011 |
| 775 | 0.823 | 1.020 | 1.011 |
| 775 | 0.853 | 1.026 | 1.013 |
| 775 | 0.932 | 1.041 | 1.011 |
| 775 | 0.980 | 1.052 | 1.012 |
| 775 | 0.854 | 1.021 | 1.011 |
| 775 | 0.887 | 1.020 | 1.009 |
| 775 | 0.873 | 1.023 | 1.011 |
| 775 | 0.857 | 1.020 | 1.010 |
| 775 | 0.815 | 1.017 | 1.010 |
| 825 | 0.875 | 1.019 | 1.010 |
| 825 | 0.849 | 1.020 | 1.010 |
| 825 | 0.912 | 1.034 | 1.012 |
| 825 | 0.970 | 1.043 | 1.011 |
| 825 | 0.953 | 1.038 | 1.012 |
| 825 | 0.844 | 1.022 | 1.012 |
| 825 | 0.921 | 1.031 | 1.012 |
| 825 | 0.897 | 1.026 | 1.011 |
| 825 | 0.902 | 1.029 | 1.012 |
| 825 | 0.827 | 1.020 | 1.010 |

*NNO transition state*. Internal co-ordinates are defined as in t*he inset in* Fig. 5 [48]. $F_D$, $F_d$ and $F_\alpha$ were varied in the same ranges as above for the *ONNO* transition state and α in the range 100–180° (in steps of 5°). The reaction co-ordinate was defined in two ways, as a) $F_{Dd} = +(F_D F_d)^{1/2}$ with $F_{dd} = 0$, and b) $F_{Dd} = -(F_D F_d)^{1/2}$ with $F_{dd} = 0$. Selected results for 775 K are presented in Fig. 5.

We are interested in those combinations of the parameters of the transition states for which the calculated values of kinetic isotope effects fall into the experimental range of 1.011 ± 0.001. Figs. 4 and 5 reveal a variety of such combinations, both for ONNO and NNO transition state. Nevertheless, if the results are analysed further, taking into account the temperature independence found experimentally, only case a) of the ONNO transition state was found to fulfil this requirement. Fig. 6 shows the dependence on temperature of two combinations for each type of transition state. In contrast to NNO, both combinations for the ONNO transition state show lack of temperature dependence. With the condition $F_{Dd} = (F_D F_d/2)^{1/2}$, an asymmetric reaction co-ordinate was defined as the simultaneous strengthening of the N–N bond and weakening of both N–O bonds. Thus, our calculations suggest a direct dissociation of dimers into $N_2$(a) + 2O(a), without an $N_2O$ intermediate as the rate-determining and

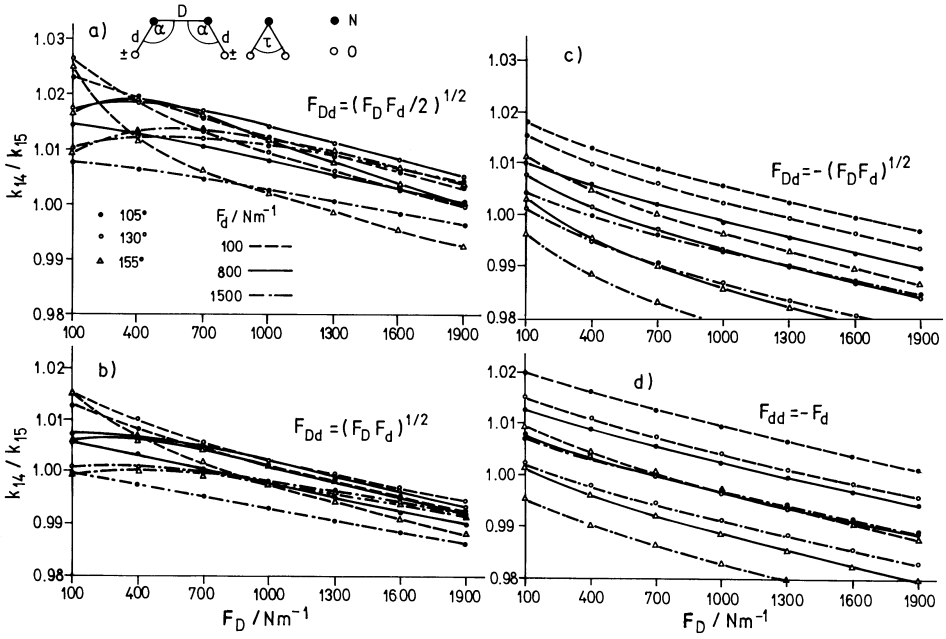


**Figure 4.** ONNO transition state: $k_{14}/k_{15}$ at 775 K *versus* $F_D$ for selected values of other parameters. Internal co-ordinates are defined as in the inset. $\tau = 0°$, $F_\alpha = 80$ Nm$^{-1}$, $F_\tau = 20$ Nm$^{-1}$. Values of $\alpha$ and $F_d$ are given in **a**).

isotope fractionation governing step, which is in agreement with our experiments, where $N_2O$ was not found in the residual gas mixture. The interbond angle $\alpha$ is limited to the range 110–130°, close to the values in the TS2 and TS3 transition states proposed by applying the B3LYP method with cc-pVTZ basis set [40]. On the other hand, a wide range of values of ($F_D$, $F_d$) pairs equally well reproduce both the absolute values and temperature independence of kinetic isotope effects. Thus, merely on the basis of our analysis, we cannot distinguish between a dimer with a very weak N–N interaction ($F_D = 100$ Nm$^{-1}$, $D = 188$ pm) and strong N–O bonds ($F_d = 1400$ Nm$^{-1}$, $d = 116$ pm), and a dimer with stronger N–N bond ($F_D = 900$ Nm$^{-1}$, $D = 128$ pm) and weaker N–O bonds ($F_d = 800$ Nm$^{-1}$, $d = 128$ pm). With reference to the TS2 and TS3 geometries mentioned above [40], the latter combination appears to be more realistic, although additional support is reviewed and expected from our quantum chemical calculations currently underway [53–55].

## CONCLUSIONS

Over the temperature range from 725 to 825 K and at initial NO pressures between 40 and 60 kPa, the reaction NO + 2Cu → 1/2 $N_2$ + $Cu_2O$ was found to be second

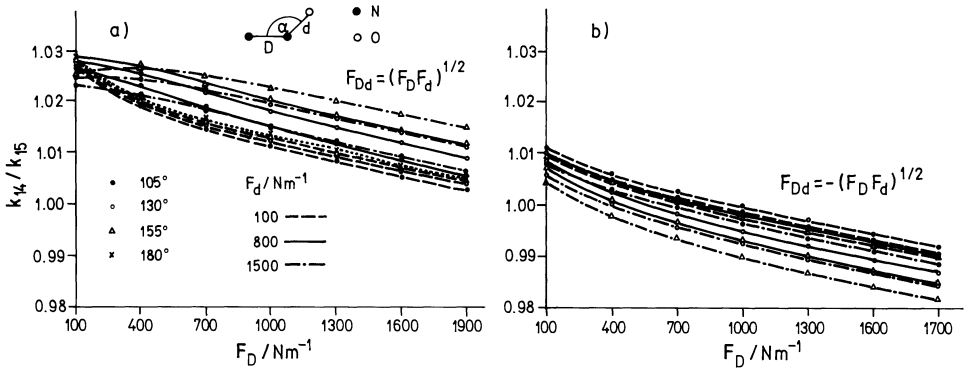


**Figure 5.** NNO transition state: $k_{14}/k_{15}$ at 775 K *versus* $F_D$ for selected values of other parameters. Internal co-ordinates are defined as in the inset. $F_\alpha = 80$ Nm$^{-1}$. Values of α and $F_d$ are indicated in **a**). For $\alpha = 180°$ (dotted line) only $F_d = 100$ Nm$^{-1}$ is shown.

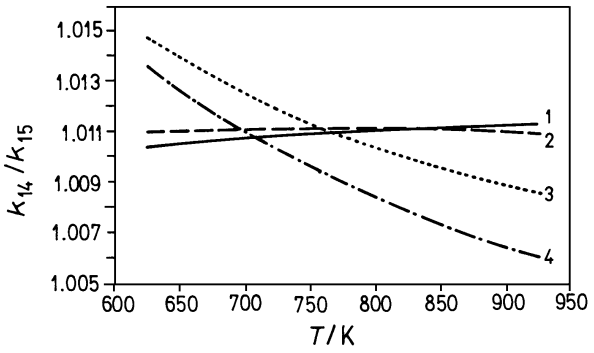


**Figure 6.** Temperature dependence of calculated $k_{14}/k_{15}$ for selected values of parameters of ONNO and NNO transition states. **1**: ONNO: $F_D = 100$ Nm$^{-1}$, $F_d = 1400$ Nm$^{-1}$, $F_{Dd} = (F_D F_d/2)^{1/2}$, $F_{dd} = 0$, $F_\alpha = 80$ Nm$^{-1}$, $F_\tau = 20$ Nm$^{-1}$, $\alpha = 130°$, $\tau = 0°$; **2**: ONNO: $F_D = 900$ Nm$^{-1}$, $F_d = 800$ Nm$^{-1}$, $F_{Dd} = (F_D F_d/2)^{1/2}$, $F_{dd} = 0$, $F_\alpha = 80$ Nm$^{-1}$, $F_\tau = 20$ Nm$^{-1}$, $\alpha = 110°$, $\tau = 0°$; **3**: NNO: $F_D = 1400$ Nm$^{-1}$, $F_d = 100$ Nm$^{-1}$, $F_{Dd} = (F_D F_d)^{1/2}$, $F_{dd} = 0$, $F_\alpha = 100$ Nm$^{-1}$, $\alpha = 130°$; **4**: NNO: $F_D = 1400$ Nm$^{-1}$, $F_d = 100$ Nm$^{-1}$, $F_{Dd} = -(F_D F_d)^{1/2}$, $F_{dd} = 0$, $F_\alpha = 80$ Nm$^{-1}$, $\alpha = 180°$.

order in NO, with no $N_2O$ intermediate observed. For theoretical interpretation of the experimental nitrogen-15 kinetic isotope effects, ONNO and NNO transition states were used. A planar *cis* ONNO with $\alpha = 130°$, $F_D = 900$ Nm$^{-1}$ and $F_d = 800$ Nm$^{-1}$, together with an asymmetric reaction co-ordinate, satisfactorily reproduces the absolute value as well as the temperature independence of $k_{14}/k_{15} = 1.011 \pm 0.001$. Neither ONNO with other reaction co-ordinates nor any NNO transition state successfully accounts for the experimental results because of too high a temperature dependence.

Acknowledgments

This study was funded by the Ministry of Education, Science and Sport of Slovenia. The authors thank Ms Lilijana Per for her figures.

## REFERENCES

1. Bertelsen B.I., *Plat. Met. Rev.*, **45**, 50 (2001).
2. Pârvulescu V., Grange P. and Delmon B., *Catal. Today*, **46**, 233 (1998).
3. Shelef M., *Chem. Rev.*, **95**, 209 (1995).
4. Nieuwenhuys B.E., *Adv. Catal*., **44**, 259 (2000).
5. Fernández-García M., Márkez Alvarez C., Rodríguez-Ramos I., Guerrero-Ruíz A. and Haller G.L., *J. Phys. Chem*., **99**, 16380 (1995).
6. Iwamoto M., Yashiro H., Mine Y. and Kagawa S., *Chem. Lett*., 213 (1989).
7. Iwamoto M., Yashiro H., Tanada K., Mizuno N., Mine Y. and Kagawa S., *J. Phys. Chem*., **95**, 3727 (1991).
8. Iwamoto M., Furukawa H. and Kagawa S., in: L. Guczi, F. Solymosi and P. Tetenyi (Eds), Proc. 10th International Congress on Catalysis, Budapest, Hungary, p.1285. Akadémiai Kiadó, Budapest (1993).
9. Iwamoto M., Furukawa H. and Kagawa S., in: Y. Murakami, A. Iijima and J.W. Ward (Eds), *New Developments in Zeolite Science and Technology, Studies in Surface Science and Catalysis*, p. 943, Elsevier Science, Amsterdam (1986).
10. Illas F., López N., Ricart J.M., Clotet A., Conesa J.C. and Fernández-García M., *J. Phys. Chem*., **102**, 8017 (1998).
11. Fernández-García M., Martínez-Arias A., Belver C., Anderson J.A., Conesa J.C. and Soria J., *J. Catal*., **190**, 387 (2000).
12. Matloob M.H. and Roberts M.W., *J. Chem. Soc. Farad. Trans. I*, **73**, 1393 (1977).
13. Johnson D.W., Matloob M.H. and Roberts M.W., *J. Chem. Soc. Chem. Commun.,* 40 (1978).
14. Johnson D.W., Matloob M.H. and Roberts M.W., *J. Chem. Soc. Farad. Trans. I*, **75**, 2143 (1979).
15. Sesselmann W., Woratschek B., Küppers J., Goyen G., Ertl G., Haberland H. and Morgner H., *Phys. Rev. Lett*., **60**, 1434 (1988).
16. Fernández-García M., Conesa J.C. and Illas F., *Surf. Sci*., **280**, 441 (1993).
17. Munakata T., Mase K. and Kinoshita I., *Surf. Sci*., **286**, 73 (1993).
18. Illas F., Ricart J.M. and Fernández-García M., *J. Chem. Phys*., **104**, 5647 (1996).
19. Rochefort A. and Fournier R., *J. Phys. Chem*., **100**, 13506 (1996).
20. van Daelen M.A., Neurock M. and van Santen R.A., *Surf. Sci*., **417**, 247 (1998).
21. van Daelen M.A., Li Y.S., Newsam J.M. and van Santen R.A., *Chem. Phys. Lett*., **226**, 100 (1994).
22. Wee A.T.S., Lin J., Huan A.C.H., Loh F.C. and Tan K.L., *Surf. Sci*., **304**, 145 (1994).
23. van Daelen M.A., Li Y.S., Newsam J.M. and van Santen R.A., *J. Phys. Chem*., **100**, 2279 (1996).
24. Dhesi S.S., Haq S., Barrett S.D. and Leibsle F.M., *Surf. Sci*., **365**, 602 (1996).
25. Dumas P., Suhren S., Chabal Y.J., Hirschmugl C.J. and Williams G.P., *Surf. Sci*., **371**, 200 (1997).
26. Takehiro N., Besenbacher F., Laegsgaard E., Tanaka K. and Stensgaard I., *Surf. Sci*., **397**, 145 (1998).
27. Ertl G., *Surf. Sci*., **6**, 208 (1967).
28. Lu H., Pradier C.-M. and Flodstörm A.S., *J. Mol. Catal. A: Chem*., **112**, 447 (1996).
29. So S.K., Franchy R. and Ho W., *J. Chem. Phys*., **95**, 13285 (1991).
30. Ohno Y., Kimura K., Bi M. and Matsushima T., *J. Chem. Phys*., **110**, 8221 (1999).
31. Dinerman C.E. and Ewing G.E., *J. Chem. Phys*., **53**, 626 (1970).
32. Eshelman D.E., Torre F.J. and Bigeleisen J., *J. Chem. Phys*., **60**, 420 (1974).
33. Zhou M. and Andrews L., *J. Phys*. *Chem. A*, **104**, 2618 (2000).
34. Nelin C., Bagus P.S., Behm J. and Brundle C.R., *Chem. Phys*. *Lett*., **105**, 58 (1984).
35. Ward T.R., Hoffmann R. and Shelef M., *Surf. Sci*., **289**, 85 (1993).
36. Tonner B.P., Kao C.M., Plummer E.W., Caves T.C., Messmer R.P. and Salaneck W.R., *Phys. Rev. Lett*., **51**, 1378 (1983).
37. Duarte H.A., Proynov E. and Salahub D.R., *J. Chem. Phys*., **109**, 26 (1998).
38. East A.L.L. and Watson J.K.G., *J. Chem. Phys*., **110**, 6099 (1999).

39. Tsurumaki H., Fujimura Y. and Kajimato O., *J. Chem. Phys*., **111**, 592 (1999).
40. Vincent M.A., Hiller I.H. and Salsi L., *Phys. Chem. Chem. Phys*., **2**, 707 (2000).
41. Lesar A. and Senegačnik M., *J. Chem. Phys*., **99**, 187 (1993).
42. Polič S., Senegačnik M., Kobal I. and Zieliński M., *Polish J. Chem*., **75**, 1729 (2001).
43. Brauer G., *Handbuch der präparativen anorganischen Chemie*, Ferdinand Enke Verlag Stuttgart (1954).
44. Bigeleisen J. and Wolfsberg M., *Adv. Chem. Phys*., **1**, 15 (1958).
45. Senegačnik M., Doctoral Thesis, Faculté des Sciences, Université de Paris, France, CEA (Commissariat à l'Energie Atomique) Report No. 726, Paris, France (1957).
46. van Hook W.A., in: C.J. Collins and N.S. Bowman (Eds), *Isotope Effects in Chemical Reactions*, Van Nostrand-Reinhold, NY, p. 1 (1970).
47. Hauffe K., *Reaktionen in und an festen Stoffen*, Springer Verlag, Berlin (1966).
48. Xemva P., Lesar A., Senegačnik M. and Kobal I., *Phys. Chem. Chem. Phys*., **2**, 3319 (2000).
49. Wilson E.B., Decius J.C. and Cross P.C., *Molecular Vibrations*, McGraw-Hill, NY, (1965).
50. Thomas T.H., Ladd J.A., Jones I.P. and Orville-Thomas W.J., *J. Mol. Struct*., **3**, 49 (1969).
51. Ladd J.A. and Orville-Thomas W.J., *Spectrochim. Acta*, **22**, 919 (1969).
52. Cioslowski J., Liu G. and Castro R.A.M., *Chem. Phys. Lett*., **331**, 497 (2000).
53. Kokalj A., *J. Mol. Graphics Mod*., **17**, 176 (1999).
54. Kokalj A., Doctoral Thesis, Faculty of Chemistry and Chemical Technology, University of Ljubljana, Ljubljana, Slovenia (2000).
55. Kokalj A., Kobal I., Horino H., Ohno Y. and Matsushima T., *Surf. Sci*., **506**, 196 (2002).